

Femtometer Displacement Resolution with Phase-Insensitive Doppler Sensing

Bethany J. Little^{1,3,*}, Julián Martínez-Rincón^{1,3**,†}, Umberto

Bortolozzo², Stefania Residori², and John C. Howell^{1,3,4,5}

¹Department of Physics and Astronomy, University of Rochester, Rochester, New York 14627, USA

²Institut de Physique de Nice, UMR7010, Université de Nice-Sophia Antipolis, CNRS, 1361 route des Lucioles, 06560 Valbonne, France

³The Center for Coherence and Quantum Optics, University of Rochester, Rochester, New York 14627, USA

⁴Institute for Quantum Studies, Chapman University, 1 University Drive, Orange, California 92866, USA

⁵Racah Institute of Physics, The Hebrew University of Jerusalem, Jerusalem 91904, Israel and

**Current address: Department of Physics, Stanford University, Stanford, California 94305, USA.

(Dated: February 9, 2018)

The measurement of extremely small displacements is of utmost importance, both for fundamental studies [1–4] and practical applications [5–7]. One way to estimate a small displacement is to measure the Doppler shift generated in light reflected off an object moving with a known periodic frequency. This remote sensing technique converts a displacement measurement into a frequency measurement, and has been considerably successful [8–14]. The displacement sensitivity of this technique is limited by the Doppler frequency noise floor and by the velocity of the moving object. Other primary limitations are hours of integration time [12, 13] and optimal operation only in a narrow Doppler frequency range.

Here we show a sensitive device capable of measuring $\mu\text{Hz}/\sqrt{\text{Hz}}$ Doppler frequency shifts corresponding to tens of fm displacements for a mirror oscillating at 2 Hz. While the Doppler shift measured is comparable to other techniques [12, 13], the position sensitivity is orders of magnitude better, and operates over several orders of magnitude of Doppler frequency range. In addition, unlike other techniques which often rely on interferometric methods, our device is phase insensitive, making it unusually robust to noise.

Remote sensing, which may be defined as the acquisition of information about an object without physical contact [15], has existed since humans first looked at objects. However the term, which first gained popularity in the 1960's [16], has been primarily used in the fields of geology and astronomy to measure relatively large scale information; Doppler measures of moving humans or birds are considered small on these scales [14, 17].

The small-displacement limits of sensing have been pushed with various reported methods. By measuring the beat frequency of a laser beam reflected of a mirror oscillating at 10 kHz, a noise equivalent displacement of 10 fm/ $\sqrt{\text{Hz}}$ after 10 s of integration time was reported [18], and similar results have been achieved with optomechanical approaches [3]. Weak-values techniques have been successful for velocity measurements in the low frequency regime of a Michelson interferometer [12, 13], reporting 60 fm/s for an oscillating mirror frequency of 2.5 mHz and an integration time of about 40 hours [13]. Non-classical light has been used to reach the fm/ $\sqrt{\text{Hz}}$ regime in MEMS cantilevers [19]. On a much larger oscillator mass scale, the LIGO collaboration reached a remarkable noise floor of about 10^{-20} m/ $\sqrt{\text{Hz}}$ for mirror oscillations of 100 Hz [1]. With a position sensitivity spanning the range from nanometers down to tens of femtometers, and

operating in an oscillator frequency regime of single Hz, this paper demonstrates a device that is both sensitive and versatile enough to place remote sensing in a new realm of ultra-small displacement measurements.

The key to the success of the experiment described here is the remarkable combination of frequency sensitivity and the phase insensitivity arising from two-wave mixing inside a highly dispersive liquid crystal light valve (LCLV) [20, 21]. In a previous work, Bortolozzo et al. [22] demonstrated that the linear dispersive regime of the LCLV can be used to measure doppler shifts down to a microhertz; here we extend this work. By using a periodic oscillating mirror movement, we are able to determine the minimum position sensitivity of the device. Using measurements of up to ten minutes, we also measure the noise spectrum of the sensor in the low frequency regime (sub-Hertz), demonstrating remarkable stability and sensitivity in a notoriously noisy frequency regime.

In our setup, shown in Figure 1, a moving piezo-driven mirror generates a Doppler shift in one beam relative to a reference beam, after which both beams interact in the LCLV. Since the LCLV is highly sensitive to small frequency shifts, we can use it to measure Doppler shifts caused by extremely small displacements of the mirror [23].

The Doppler shift of light incident at 45° on a mirror moving with a velocity v_m is given by $f_d = \sqrt{2}v_m/\lambda$, where λ is the wavelength of the light. If the mirror follows a harmonic oscillation with amplitude A and frequency f_m , then the maximum Doppler shift induced in

* bethanyjeanlittle@gmail.com

† The first two authors contributed equally to this work.

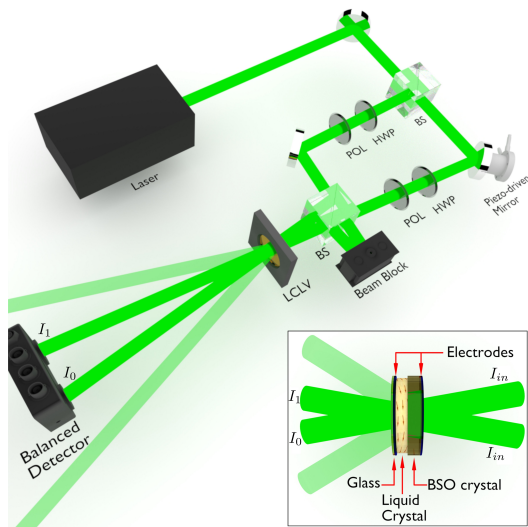


FIG. 1. Diagram (not to scale) of the experimental setup. A laser of wavelength 532 nm is divided by a beamsplitter (BS). One beam is Doppler shifted by reflecting off a moving piezo-driven mirror, and is incident with the unshifted beam on the LCLV. The first-order output beams with intensities I_0 and I_1 are incident on a balanced detector, and the sum and difference are measured. Polarizer (POL) and half-wave plate (HWP) combinations control the power and polarization of each beam. The inset shows the components of the LCLV. A photorefractive layer (BSO) on the entrance face and a glass plate on exit face hold in place the liquid crystal layer. Transparent electrodes are used to apply an external bias voltage which enables tuning of the response of the device. The angle of 0.3 degrees between the two beams incident on the LCLV is exaggerated. A combination of lenses and irises (not shown) are used to focus the first orders onto the detector and filter out the higher orders produced by the wave mixing into the LCLV.

the reflected light is

$$f_d = \sqrt{2}kA f_m, \quad (1)$$

where $k = 2\pi/\lambda$ is the wavenumber.

We now give a brief description of the LCLV and its expected frequency response. The LCLV derives its unique properties from the combination of a liquid crystal layer and a photorefractive layer. The photorefractive layer is an inorganic bismuth silicate crystal ($\text{Bi}_{12}\text{SiO}_{20}$), transparent in the visible range. This acts as one side of a cell wall for the liquid crystal, which is held in place on the other side by a glass (BK7) window, as shown in the inset of Figure 1. Spacers a few microns long define the thickness of the liquid crystal. Transparent electrodes placed within the crystal sandwich allow tuning of the LCLV's properties by means of an applied AC voltage.

The index of refraction of the liquid crystal varies dramatically depending on the orientation of its long molecules, which rotate according to the potential difference between the plates. Light incident on the bismuth silicate crystal creates an intensity dependent spatial modification of the effective voltage across the liquid

crystal layer. This causes the molecules of the liquid crystal to rotate locally, creating a spatially dependent index [24].

When two beams of equal intensity I_{in} and wave vectors \vec{k}_1 and \vec{k}_2 are incident on the device, their combined field creates a grating within the LCLV, with grating wave vector $\vec{K}_g = \vec{k}_1 - \vec{k}_2$. The grating allows energy exchange between the beams; the interaction may be viewed as a wave mixing process. If the periodicity of their interference, $\Lambda \equiv 2\pi/K_g$, is much greater than the thickness d of the liquid crystal, the diffracted orders of the output can be characterized according to nonlinear wave mixing in the Raman-Nath regime [24]. This two-beam process has been shown to have remarkably slow group velocities [20], and corresponding group delays τ on the order of hundreds of milliseconds over only a few microns of material.

The m^{th} order output intensity of the wave mixing is given by [25]

$$\frac{I_m}{I_{in}} = |J_{m-1}(\rho) + iJ_m(\rho)e^{-i\Psi}|^2 \quad (2)$$

where $\tan \Psi = f_d\tau / (1 + l_d^2 K_g^2)^2$, and J_m denote the Bessel functions of the first kind, with argument

$$\rho = \frac{2kn_2 I_{in} d}{\sqrt{(1 + l_d^2 K_g^2)^2 + (f_d\tau)^2}}. \quad (3)$$

Here n_2 is the equivalent Kerr-type nonlinear index, and l_d is the transverse diffusion length, determined by the material constants and the applied AC voltage [26] (See Methods). The normalized intensity difference between the zeroth and first-order beams is a function of the frequency difference between them and is given by

$$\frac{\Delta I}{I_{in}} = \frac{I_1(f_d) - I_0(f_d)}{I_{in}} \quad (4)$$

For small Doppler frequency shifts, there is a linear response,

$$\Delta I \approx f_d \chi I_{in}, \quad (5)$$

the slope of which can be calculated as [22]

$$\chi = 8\pi\tau J_0(2kdn_2 I_{in}) J_1(2kdn_2 I_{in}). \quad (6)$$

The value of χ is dependent on a variety of experimental parameters, including the group index, which is related to τ , the nonlinear Kerr coefficient n_2 , and the intensities of the beams incident on the LCLV. For our experiment, χ is estimated to be 0.5 s (see Methods).

We note that, unlike common interferometric methods for measuring small frequency shifts and displacements, the amplitude of our signal does not depend on the relative phase between the two beams. This is similar to other wave mixing processes, such as inside acousto-optic modulators. The large linear response χ and this phase insensitivity are the major advantages of using a LCLV.

The experimental setup is shown in Figure 1. Collimated light from a laser at 532 nm is split on a 50/50 beamsplitter, and one beam reflects off a piezo-driven (PI S310) mirror and experiences a Doppler shift relative to the other beam. A Mach-Zehnder type setup is used to create a slight angle between the two beams on the order of 0.3 degrees, and both beams are then incident on the LCLV. Note that the two beams do not recombine on the beamsplitter before the LCLV. The small angle between the beams ensures that the interaction occurs in the Raman-Nath regime [24, 27, 28]. The two primary diffracted output orders of the LCLV are focused onto a balance detector (Thorlabs PDB210A2/M). Irises are used to block light from the higher diffracted orders.

In order to minimize noise due to turbulence, temperature drifts, and room light, the apparatus is enclosed inside an insulating foam box. The optical table is not floated and no further isolation measures are used, an indication of the remarkable stability of this technique. For small Doppler shifts, a lock-in amplifier is used to measure the signal from the balance detector, which is fed through a high pass filter to avoid overload of the lock-in due to DC drifts. For measurement of the noise spectrum (Figure 2) no filtering is used.

The LCLV used has a thickness $d = 9 \mu\text{m}$, a group delay $\tau = 72 \text{ ms}$, and is optimized by a 2.6 V AC driving voltage at 1kHz, giving an estimated effective nonlinear index $n_2 = -1.8 \times 10^{-4} \text{ W/m}^2$, $l_d \approx 12 \mu\text{m}$, and linear response $\chi = 0.5 \text{ s}$. The beams at the LCLV have a $1/e^2$ diameter of 4 mm, and the interference spacing is $\Lambda \approx 110 \mu\text{m}$. The mirror is modulated at a fixed frequency of 2 Hz, with an amplitude determined by the applied voltage and the manual-specified piezo response of 60 nm/V.

The results of the device depend on both the noise floor and the linearity of the response. We analyze both of these criteria, and follow with a discussion of the range and practicality of the device.

The fundamental noise limit for laser power measurements using a coherent source is given by the shot noise \sqrt{N} . Using equation (5), and writing the power P in terms of the photon number N by using the energy per photon, hc/λ , we find the limit for measuring a frequency shift with this device,

$$f_{SN} = \frac{1}{\chi} \sqrt{\frac{1}{N}} = \frac{1}{\chi} \sqrt{\frac{hc}{\eta \lambda P T}}, \quad (7)$$

where η is the detector efficiency and T is the acquisition time per measurement.

The limit of Equation (7) is plotted in Figure 2 along with the measured noise spectrum for the device when the mirror is driven at 2 Hz. We normalize the spectrum using a reference signal of 100mV on the piezo, which gives a Doppler shift of 200 mHz. The spectrum was obtained by taking the finite Fourier transform of a 10 minute scan, with no electrical or frequency filtering. The power incident on the detector is 1.15 mW, and the detector efficiency is $\eta = 0.35$ giving, for our experimental parameters, a shot noise limit of $f_{SN} = 60 \text{ nHz}/\sqrt{\text{Hz}}$.

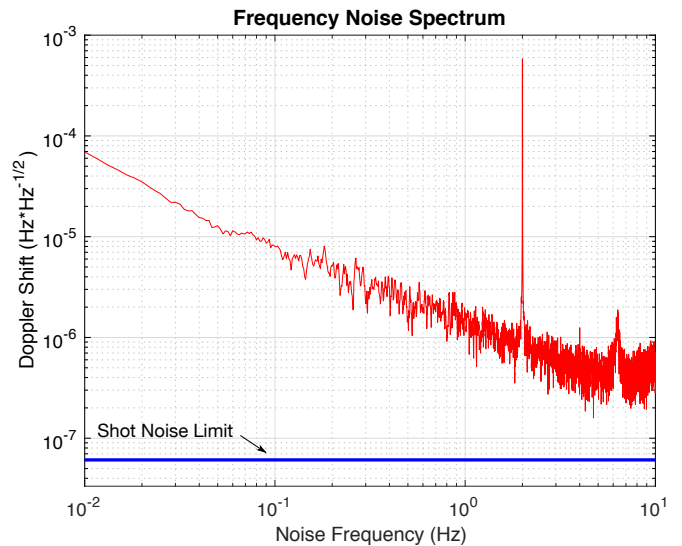


FIG. 2. Noise spectrum for the device, with a 100 mV reference signal at 2 Hz applied to the piezo stack. We obtained the spectrum by taking a FFT of a 10 minute scan. The reference signal, which corresponds to a Doppler shift of 200 mHz, is used to normalize the vertical axis. The spectrum is shown up to the bandwidth of the linear region of the LCLV, around 10 Hz. The blue line is the SNL based on the estimated value of χ . At 2 Hz, the noise floor is around $1 \mu\text{Hz}/\sqrt{\text{Hz}}$; for a mirror oscillating at 2 Hz, this corresponds to a displacement sensitivity of around $20 \text{ fm}/\sqrt{\text{Hz}}$.

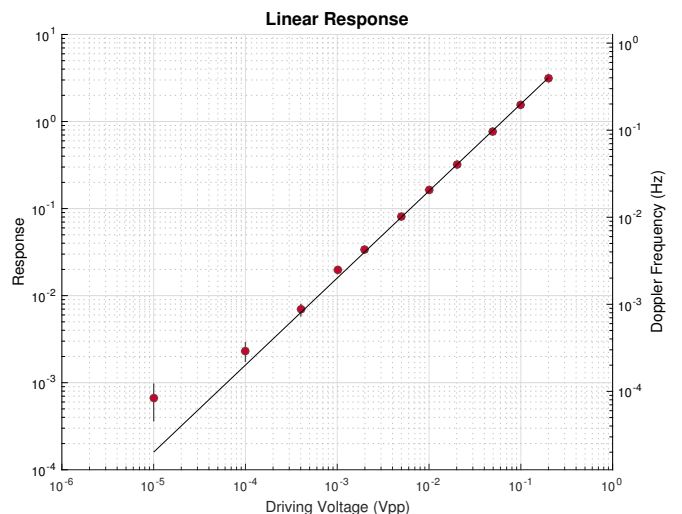


FIG. 3. The difference signal at the detector is shown as a function of the peak to peak amplitude of the the voltage applied to the piezo. The response is linear above 10^{-4} V . The black line is the theoretical linear response. At low voltages, the electronics of the piezo driver become nonlinear and the applied voltage from the driver is no longer equal to the voltage on the piezo.

In order to obtain the normalization of Figure 2, the reference signal must be well within the linear response region of the device. Figure 3 shows the measured response of the LCLV for different applied Doppler shifts, generated by a signal at 2 Hz and with varying peak-to-peak voltages. The linear response is evident for voltages above $10^{-4} V_{pp}$. The nonlinear response of the electronics driving the piezo limit the application of smaller voltages, and result in divergence from the expected linear behavior. The reference signal at 200 mHz, however, is well within the linear region. The data in Figure 5 in the Methods Section also confirms that the reference signal is within the linear response region.

We find the shot noise limited displacement using Equations (1) and (7):

$$A_{SN} = \frac{1}{\sqrt{2k}f_m} f_{SN} = \frac{1}{kf_m\chi} \sqrt{\frac{hc}{2\eta\lambda PT}}. \quad (8)$$

Since the displacement of the mirror can be calculated as a function of the measured Doppler shift according to Eq. (1), the sensitivity of the device is correspondingly proportional:

$$\delta A = \frac{1}{\sqrt{2k}} \frac{\delta f_d(f_m)}{f_m}. \quad (9)$$

Here δA is the position sensitivity, and δf_d the Doppler sensitivity. This relationship is used to plot the noise spectrum for position in Figure 4. For our experimental parameters, $A_{SN} = 1.8 \text{ fm}/\sqrt{\text{Hz}}$. Figure 2 shows a Doppler sensitivity at our reference mirror frequency of 2 Hz to be around $1 \mu\text{Hz}/\sqrt{\text{Hz}}$. The corresponding displacement noise floor, shown in Figure 4 is calculated to be around $20 \text{ fm}/\sqrt{\text{Hz}}$, which is only about an order of magnitude above the shot noise limit.

To better compare our results to other Doppler measures, we may also consider the velocity of the moving mirror, given by $v_m = f_d\lambda/\sqrt{2}$. Considering the measured noise floor in Figure 2 to be $\mu\text{Hz}/\sqrt{\text{Hz}}$, the corresponding measurable velocity is $400 \text{ fm/s}/\sqrt{\text{Hz}}$. This is similar to the result found in Ref [12]; however in their case the measurement was achieved by averaging about two hours worth of data; in ours this is the sensitivity per $\sqrt{\text{Hz}}$. Even one hour of integration time with our device gives, according to equation (7), a shot-noise limited velocity measurement of 6 fm/s . Using a combination of balance detection and weak values, sensitivities as small as 60 fm/s have recently been reported [13]; however this was only after 40 hours of integration time. Thus we see that not only is our technique comparable to other precision velocity measurements, but it is also vastly more robust.

We have proposed and demonstrated a remote sensing technique which makes use of a LCLV to measure Doppler shifts and corresponding displacements with a noise floor on the order of $20 \text{ fm}/\sqrt{\text{Hz}}$ in the Hz regime. Direct measurement of displacements this small were limited not by the device, but by the nonlinearity of the piezo

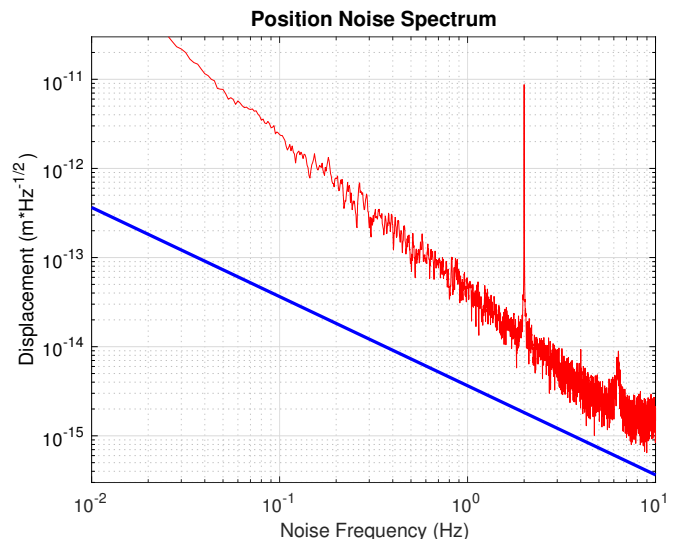


FIG. 4. The noise spectrum for position measurement, calculated from the spectra of Figure 2, is plotted. The blue line is the shot noise-limited sensitivity for position measurement from Equation (9). For a mirror frequency of 2 Hz, the noise is around $20 \text{ fm}/\sqrt{\text{Hz}}$, which is only about an order of magnitude above the calculated shot noise limit of $1.8 \text{ fm}/\sqrt{\text{Hz}}$ at that frequency.

and driver for low voltages. In principal, without this added noise in the moving object, the LCLV measuring device is linear down to arbitrarily small measurements, and is limited only by the noise floor of the measurement. The Doppler frequency noise floor of the technique, measured to be around $\mu\text{Hz}/\sqrt{\text{Hz}}$, is only about an order of magnitude above the shot noise limit, remarkable for a tabletop experiment with no isolation, damping, or filtering.

Many other measurement techniques operate in a higher frequency regime, where it is not only easier to obtain higher precision by averaging, but also typically easier to approach the shot noise limit. In contrast, our device is optimized to work at 2 Hz, a frequency regime of great interest, for instance to the gravitational-wave community [29]. This optimal frequency range of the device is set primarily by the thickness of LCLV. We plan to investigate working at even lower frequencies by tuning the thickness and driving voltages of LCLVS to optimize their behavior at low frequency.

We believe this new regime of remote sensing will have many novel applications. For example, we anticipate the LCLV could be used for micro-mechanical cooling applications where it has proved difficult to measure the ground state. The range could be useful in biological applications in bridging the gap toward increasingly smaller scales. Finally, in a return to the original motivation for the development of liquid crystals, and in line with the history of remote sensing, we plan to explore the femtometer scale imaging capabilities of the LCLV.

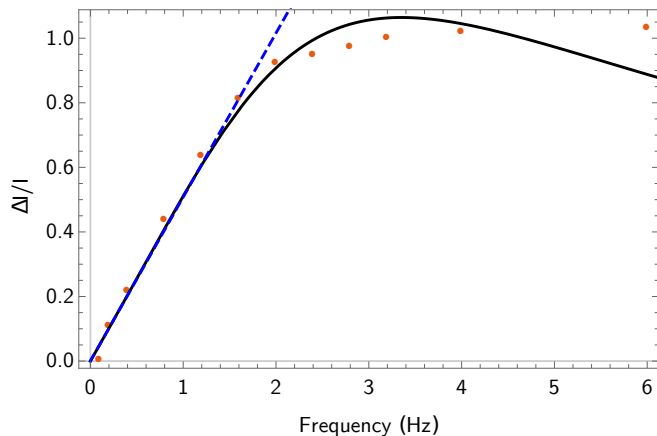


FIG. 5. Data (red dots) and fit (black) used to estimate the value of the slope χ of the linear region (see dashed line). The fit yields $\chi = 0.5$ s.

I. ACKNOWLEDGEMENTS AND FUNDING

This work is supported by the Direction Générale de l’Armement (DGA), under the contract ANR-14-ASMA-0004-01, Astrid Maturation HYDRE, the Army Research Office (ARO) (W911NF-12-1-0263), and Northrop Grumman Corporation.

II. METHODS

A. Determination of χ

An estimate of χ may be obtained by generating increasingly large frequency shifts between the two beams to determine the end of the linear region of the response curve. Fitting this response to the full expression for the expected response allows determination of n_2 and calculation of χ using Equation (6). Figure 5 shows the data (red circles) and theory fit for this calculation, as well as the slope $\chi = 0.5$ s of the linear region (blue, dashed line).

B. Diffusion Length

The transverse diffusion length is

$$l_d = \frac{d\sqrt{\Delta_\epsilon/K}}{V}, \quad (10)$$

where Δ_ϵ is the dielectric anisotropy, K is the elastic constant of the liquid crystal, V is the AC voltage applied to the liquid crystal, and d is the thickness of the cell.

The diffusion length l_d is determined by observing the point spread function. Light is tightly focused on the BSO crystal, which induces a refractive index variation δn of the same shape as the light spot, but of different transverse size; this transverse index variation gives l_d . For our cell, $l_d \approx 12$ microns.

-
- [1] BP Abbott, Richard Abbott, TD Abbott, MR Abernathy, Fausto Acernese, Kendall Ackley, Carl Adams, Thomas Adams, Paolo Addesso, RX Adhikari, et al., “Observation of gravitational waves from a binary black hole merger,” *Physical review letters* **116**, 061102 (2016).
 - [2] Thomas Corbitt, Yanbei Chen, Edith Innerhofer, Helge Müller-Ebhardt, David Ottaway, Henning Rehbein, Daniel Sigg, Stanley Whitcomb, Christopher Wipf, and Nergis Mavalvala, “An all-optical trap for a gram-scale mirror,” *Phys. Rev. Lett.* **98**, 150802 (2007).
 - [3] Markus Aspelmeyer, Tobias J. Kippenberg, and Florian Marquardt, “Cavity optomechanics,” *Rev. Mod. Phys.* **86**, 1391–1452 (2014).
 - [4] Jasper Chan, TP Mayer Alegre, Amir H Safavi-Naeini, Jeff T Hill, Alex Krause, Simon Gröblacher, Markus Aspelmeyer, and Oskar Painter, “Laser cooling of a nanomechanical oscillator into its quantum ground state,” *Nature* **478**, 89–92 (2011).
 - [5] Diego Pierrottet, Farzin Amzajerdian, Larry Petway, Bruce Barnes, and George Lockard, “Flight test performance of a high precision navigation doppler lidar,” in *SPIE Defense, Security, and Sensing (International Society for Optics and Photonics, 2009)* pp. 732311–732311.
 - [6] Arnaud Peigné, Umberto Bortolozzo, Stefania Residori, Stéphanie Molin, Vincent Billault, Pascale Nouchi, Daniel Dolfi, and Jean-Pierre Huignard, “Adaptive interferometry for high-sensitivity optical fiber sensing,” *Journal of Lightwave Technology* **34**, 4603–4609 (2016).
 - [7] Valeria Levi, QiaoQiao Ruan, and Enrico Gratton, “3-d particle tracking in a two-photon microscope: application to the study of molecular dynamics in cells,” *Biophysical journal* **88**, 2919–2928 (2005).
 - [8] PAWEŁ R Kaczmarek, Tomasz Rogowski, Arkadiusz J Antonczak, and Krzysztof M Abramski, “Laser doppler vibrometry with acoustooptic frequency shift,” *Optica Applicata* **34**, 373–384 (2004).
 - [9] Lorenzo Scalise, Yanguang Yu, Guido Giuliani, Guy Plantier, and Thierry Bosch, “Self-mixing laser diode velocimetry: application to vibration and velocity measurement,” *IEEE Transactions on Instrumentation and Measurement* **53**, 223–232 (2004).
 - [10] Jocelyne Guéna, Ruoxin Li, Kurt Gibble, Sébastien Bize, and André Clairon, “Evaluation of doppler shifts to improve the accuracy of primary atomic fountain clocks,” *Phys. Rev. Lett.* **106**, 130801 (2011).
 - [11] Alexander H Meier and Thomas Roesgen, “Imaging laser doppler velocimetry,” *Experiments in fluids* **52**, 1017–1026 (2012).
 - [12] Gerardo I Viza, Julián Martínez-Rincón, Gregory A Howland, Hadas Frostig, Itay Shomroni, Barak Dayan,

- and John C Howell, “Weak-values technique for velocity measurements,” *Optics letters* **38**, 2949–2952 (2013).
- [13] Julián Martínez-Rincón, Zekai Chen, and John C Howell, “Practical advantages of almost-balanced-weak-value metrological techniques,” *Physical Review A* **95**, 063804 (2017).
- [14] Dave Tahmouh, “Review of micro-doppler signatures,” *IET Radar, Sonar & Navigation* **9**, 1140–1146 (2015).
- [15] Charles Elachi and Jakob J Van Zyl, *Introduction to the physics and techniques of remote sensing*, Vol. 28 (John Wiley & Sons, 2006).
- [16] James B Campbell and Randolph H Wynne, *Introduction to remote sensing* (Guilford Press, 2011).
- [17] Victor C Chen, “Micro-doppler effect of micromotion dynamics: a review,” in *AeroSense 2003* (International Society for Optics and Photonics, 2003) pp. 240–249.
- [18] M Weksler, Z Vager, and G Neumann, “Measurement of a very high displacement sensitivity of the beat frequency in an he-ne laser,” *IEEE Journal of Quantum Electronics* **16**, 785–790 (1980).
- [19] Raphael C Pooser and Benjamin Lawrie, “Ultrasensitive measurement of microcantilever displacement below the shot-noise limit,” *Optica* **2**, 393–399 (2015).
- [20] S. Residori, U. Bortolozzo, and J. P. Huignard, “Slow and fast light in liquid crystal light valves,” *Phys. Rev. Lett.* **100**, 203603 (2008).
- [21] U. Bortolozzo, S. Residori, and J.-P. Pierre Huignard, “Slow and fast light: basic concepts and recent advancements based on nonlinear wave-mixing processes,” *Laser and Photonics Reviews* **4**, 483–498 (2010).
- [22] Umberto Bortolozzo, Stefania Residori, and John C. Howell, “Precision doppler measurements with steep dispersion,” *Opt. Lett.* **38**, 3107–3110 (2013).
- [23] Umberto Bortolozzo, Stefania Residori, and Jean-Pierre Huignard, “Transmissive liquid crystal light-valve for near-infrared applications,” *Applied optics* **52**, E73–E77 (2013).
- [24] U Bortolozzo, S Residori, and J P Huignard, “Beam coupling in photorefractive liquid crystal light valves,” *Journal of Physics D: Applied Physics* **41**, 224007 (2008).
- [25] U. Bortolozzo, S. Residori, and J. P. Huignard, “Tuning the group delay of optical wave packets in liquid-crystal light valves,” *Phys. Rev. A* **79**, 053835 (2009).
- [26] J Prost, *The physics of liquid crystals*, 83 (Oxford university press, 1995).
- [27] NS Nagendra Nath, “The diffraction of light by supersonic waves,” in *Proceedings of the Indian Academy of Sciences-Section A*, Vol. 8 (Springer, 1938) pp. 499–503.
- [28] MG Moharam and L Young, “Criterion for bragg and raman-nath diffraction regimes,” *Applied optics* **17**, 1757–1759 (1978).
- [29] Pau Amaro-Seoane, Sofiane Aoudia, Stanislav Babak, Pierre Binetruy, Emanuele Berti, Alejandro Bohe, Chiara Caprini, Monica Colpi, Neil J Cornish, Karsten Danzmann, et al., “Low-frequency gravitational-wave science with elisa/ngo,” *Classical and Quantum Gravity* **29**, 124016 (2012).